

CONF-740529-2

LA-UR-74-1420

MASTER

TITLE: OPTICAL DESIGN AND ANALYSIS OF CARBON DIOXIDE LASER FUSION SYSTEMS USING INTERFEROMETRY AND FAST FOURIER TRANSFORM TECHNIQUES

AUTHOR(S): V. K. Viswanathan, L-1

**SUBMITTED TO: LASL Conference on Optics '79
Los Alamos, NM 87545
May 23 - 25, 1979**

NOTICE
This report was prepared as an account of work sponsored by the United States Government. Neither the United States nor the United States Government, neither the United States Department of Energy, nor any of their employees, nor any of their contractors, subcontractors, or their employees, make any warranty, express or implied, or assumes any legal liability or responsibility for the accuracy, completeness or usefulness of any information, apparatus, product or process disclosed, or represents that its use would not infringe privately owned rights.

University of California

By acceptance of this article, the publisher recognizes that the U.S. Government retains a nonexclusive, royalty-free license to publish or reproduce the published form of this contribution, or to allow others to do so, for U.S. Government purposes.

The Los Alamos Scientific Laboratory requests that the publisher identify this article as work performed under the auspices of the U.S. Department of Energy

UNCLASSIFIED



LOS ALAMOS SCIENTIFIC LABORATORY

Post Office Box 1663 Los Alamos, New Mexico 87545

An Affirmative Action/Equal Opportunity Employer

OPTICAL DESIGN AND ANALYSIS OF CARBON DIOXIDE LASER FUSION SYSTEMS
USING INTERFEROMETRY AND FAST FOURIER TRANSFORM TECHNIQUES*

V. K. Viswanathan
University of California
Los Alamos Scientific Laboratory
Los Alamos, NM 87545

Abstract

The optical design and analysis of the LASL carbon dioxide laser fusion systems required the use of techniques that are quite different from the currently used method in conventional optical design problems. The necessity for this is explored and the method that has been successfully used at Los Alamos to understand these systems is discussed with examples. This method involves characterization of the various optical components in their mounts by a Zernike polynomial set¹ and using fast Fourier transform techniques to propagate the beam, taking diffraction and other nonlinear effects that occur in these types of systems into account. The various programs used for analysis are briefly discussed.²

Introduction

The LASL CO₂ laser fusion systems resemble conventional electro-optical systems that form an aerial image in the focal plane and also have a lot in common with typical laser optical systems. The correspondence with image-forming conventional electro-optical systems arises from the fact that there are afocal and focusing subsections in the CO₂ laser fusion systems, and spatial filters are used to clean up the beam in a fashion similar to those in typical laser systems. In most of the conventional optical systems, the emphasis is on optimization of the optical transfer function properties and the tolerance analysis is based on fairly well-understood departures from the nominal situation for the optical components and the misalignments. In CO₂ laser fusion systems, the focusing properties of an optical system, like the Strehl ratio, irradiance and encircled energy distributions are relevant parameters of interest. These systems invariably are nominally diffraction-limited and the departures in performance from the ideal situation are caused by (1) the large components like the sixteen-inch sodium chloride windows; the micromachined mirrors, etc., which are not made by the conventional polishing processes and hence exhibit different imperfections from the conventional optical elements; (2) the possible nonlinear effects which can affect the phase and intensity of the beam.

Further, the LASL CO₂ laser fusion systems present some unique problems that prevent conventional techniques (dependent on ray tracing used in optical design programs) being used in an effective fashion. Some of these problems are (1) tight spatial filters are used in the CO₂ laser fusion systems and methods based on ray tracing cannot handle this situation properly. (2) There are large enough separations between components that diffraction propagation of aberrated beams has to be explicitly taken into account. (3) State-of-the-art novel components like diamond-point turned optical elements and sixteen-inch sodium chloride windows, which contribute heavily to the deterioration of the optical quality of the beam, have to be properly accounted for. Representation of these surfaces by aspheric terms or trigonometric functions or a combination of them appears inadequate and it is not obvious how easily one can represent them in an efficient fashion using spline fit surfaces. (4) High and low Fresnel numbers are encountered at different parts of the systems. (5) Nonlinear effects in the system which result in phase and the intensity of the beam being altered spatially have to be taken into proper account. (6) Existing programs which are capable of handling some of the peculiar problems of CO₂ laser fusion systems are proprietary and prohibitively expensive to use and are not capable of running in a streamlined fashion.

As a consequence, it became necessary to consider an approach (based on a combination of programs), which was custom-tailored to CO₂ laser fusion systems. The next section describes the procedure that evolved and briefly describes the programs. Subsequent sections give examples of how this procedure was used to predict and analyze the performance characteristics of these systems.

*Work performed under the auspices of the U. S. Department of Energy.

Description of the Procedure and the Various Programs
Used in the Analysis

It became quite clear that the proper representation and characterization of the optical components in the system was essential to analyze and understand the optical performance of the system. It also became obvious that the diffraction propagation of a coherent beam had to be taken into account, representation of each element by a method which enabled a good connection with the well known aberrations in conventional optical design, engineering and manufacturing is desirable. One practical interface is to deal with the optical path differences (OPD) introduced by each optical element. However, just a map of the OPD in many instances is not enough to provide the physical insight as to the role that component is playing in the overall optical performance of the system. On the other hand, use of a polynomial set like the Zernike polynomials results in an understanding of the role played by each component.³ Consequently, the choice was a method which could use either the OPD (which is capable of better accuracy) or the Zernike polynomial set (which provides better insight).

In practice, the program FRINGE fits this scheme perfectly. Fizeau or Twyman-Green interferograms at .633 microns wavelength are made of the actual manufactured components. These are digitized using the program CDFL and serve as input data to FRINGE. FRINGE uses a global polynomial to represent the fringe data, which has the general form:

$$Z = a_0 + a_1 f_1(x,y) + a_2 f_2(x,y) + \dots + a_n f_n(x,y),$$

where n is the number of terms and $f_n(x,y)$ is the Zernike polynomial in two dimensions. The maximum number of terms currently used in the program is 36. The fitting is done using the method of least squares and the minimization results in a system of linear equations. These are solved by the use of a modified Gram-Schmidt method of constructing orthogonal polynomials.⁴ Zernike polynomials at 10.6 microns are computed for each component and stored in a file called ABR. These serve as input to the diffraction propagation program LOTS.

LOTS has been designed to compute the performance of the LASL CO₂ laser fusion systems in terms of beam quality and energy. The laser pulse is treated as a two dimensional complex amplitude distribution. The principal operations performed on this distribution include: 1) diffraction propagation; 2) propagation through aberrated optical components, which can be represented by the Zernike polynomial set data reduced from interferograms or in the form of random wavefronts of specified statistics; 3) propagation through spatial filters; 4) propagation through nonlinear amplification and absorption regions; 5) propagation through clear apertures of arbitrary shape.

In principle it is similar to the system optical quality code originally developed by Siegman and Sziklas to deal with the propagation of high-energy laser beams. However, LOTS is custom tailored to the LASL CO₂ laser fusion systems and the version discussed here uses a 64 x 64 matrix and runs in about 52,000 octal versus an estimated minimum of 140,000 octal for most systems optical quality codes. LOTS runs through one entire leg of the Helios system, consisting of approximately 100 optical components in about 20 seconds on the CDC6600. This low core and fast execution time makes it quite convenient to use. A larger version which allows higher resolution of diffraction detail by the use of very large matrices is currently in the process of being implemented at Los Alamos. LOTS propagates the complex valued wavefront using diffraction calculations and represents the laser pulse as a two-dimensional complex array. It should be pointed out that the finite temporal width of the pulse is not treated, since only the spatial variations in the wavefront are of interest in optical design and engineering situations. The wavefront computations proceed from the oscillator through the various optical components (as represented by their respective Zernike polynomial set or as random wavefronts of specified statistics), spatial filters, amplifying media, (gain is computed using the Franz-Nordvik equations or the results of the LASL rate equation codes), saturable absorbers, and clear apertures as they sequentially occur in the actual system, thus directly simulating the optical train from end to end. The Strehl ratio, the encircled energy and irradiance distributions can be printed out at any of the stations in the chain. The intensity distribution of the laser beam is displayed by isometric plots or by grey scale maps. The phase of the wavefront can be displayed in the form of interferograms or phase maps.

To briefly summarize the procedure, the optical components are characterized interferometrically. Fizeau or Twyman-Green interferograms of the components are made at 633 nm wavelength. These are digitized using CDFL. The Zernike polynomial coefficients at 10.6 μ m are generated using FRINGE, and these are used to characterize the optical path difference introduced at each manufactured surface. The wavefront is propagated from end to end using LOTS, taking diffraction, nonlinear effects, and OPD modifications introduced by each component into account. The various parameters of interest, such as the

Strehl ratio, the irradiance and encircled energy distributions, the amplitude and phase of the wavefront, etc., are computed and displayed as desired.

Optical Analysis of the Helios CO₂ Laser Fusion System

The Helios system, currently operational, has delivered more than 10 kJ in a 0.5 nanosecond pulse. This system has been analyzed from end to end using the techniques described earlier in this paper. A few representative examples which illustrate the ways in which optical engineering and design decisions can be made are discussed in this section.

Figure 1 shows the optical schematic of one of the eight beams in the Helios system (the other seven beams are optically similar). Briefly, a nominal nanosecond pulse is switched out of a TEA oscillator and undergoes three stages of TEA preamplification and beam splitting before entering the final amplifiers. Each of the beams is then amplified to nearly 1400 joules from a roughly 100 mJ input. Figure 2 shows the optical schematic and the beam path through one of the final amplifiers. Optically, the final amplifier is a triple pass, 17% afocal off-axis Gregorian telescope. A 100 mJ, nearly 2 cm collimated beam increases in energy to nearly 3 joules in the first pass, strikes a turning mirror and is focused at the spatial filter. The beam then diverges and is deflected by another flat turning mirror and its energy in this second diverging pass reaches 300 joules. The beam diameter increases to roughly 34 cm and after double passing the saturable absorber cell and its salt window* and being recollimated, the energy is reduced to about 150 joules. After the third amplification pass, the energy in the collimated beam may reach nearly 1400 joules. The collimated beam is then brought to focus at the target by a turning mirror paraboloid combination. Figure 3 shows a plot of the Strehl ratio throughout the system. The curve labeled "NORMAL" represents the nominal case in which each of the optical components were essentially assumed to conform to the specifications for each component (a random peak-to-valley surface error of 0.1 λ at 10.6 microns). Other factors like the mounts, etc., do not contribute further to the optical path difference errors introduced by the elements. Further analysis showed that as long as the spatial filter 3** after which the large optical elements occur in the system is tight,† the optical elements preceding it have very little effect on the optical quality†† of the beam after passing through this spatial filter. The Strehl ratio is very close to that of a perfect beam (.98). As a consequence, the subsequent analysis shifted to the large optical elements in the chain after the last spatial filter. Figure 4 shows the system optical description of the triple-pass amplifier shown in Figure 2.

An analysis whose aim was to study and locate the critical factors which can contribute to the degradation of the optical quality of the beam at the target (as well as to predict the expected optical performance of the system), was initiated. The results are shown in Figure 5.‡ The curve (A) represents the optical performance of the nominal case in which the optical components conformed to the specifications (each component was allowed an 0.1 λ random peak-to-valley surface error at 10.6 microns) and other possible sources of error like those introduced by the mounts, possible misalignments, etc., were not taken into account. (B) represents an attempt to study the effects of aberrations introduced by the mounts, as well as to locate the critical elements in the chain. Using a rule-of-thumb criterion, it was assumed that these factors contributed an equal amount to the existing aberrations described in (A). (C) describes an actual case in which all the elements were represented by the Zernike polynomial coefficients at 10.6 microns. These coefficients were obtained by the digitization and reduction of the interferograms of the actual manufactured components in their mounts.

The nominal case (A) represents a good system, especially considering the complexities of the system. The goal is to reach that level. Referring to Figure 5, and the results for (B), it became clear that the mounts should contribute as little further aberrations as possible. As a consequence, standard commercially available mounts which likely contribute the amounts of aberrations represented in (B) were unacceptable. Comparing (A) and (C), considering elements 3 through 6, the rms values in (C) are three times larger for the 45° turning mirror and 2.2 times larger for the first pass through the saturable absorber cell salt window than those in (A), and equal for the collimating mirror. Yet, the Strehl ratio for the two cases just after the collimating mirror is almost identical (.79 for (A) and .77 for (C)). Considering the elements 5 through 11 (from the collimating mirror onwards), the collimating mirror (5), the 45° turning mirror (10), and the focusing parabola (11) have almost identical rms wavefront error values.

†Element 5 in Figure 2.

**Which is the last spatial filter in the system.

†Of the order of one Airy disc diameter.

††Even if they are twice as bad as the specifications.

The differences in rms wavefront error values are significant only in the case of the three salts. At the target plane, the Strehl ratio is 0.49 for (A) and 0.2 for (C). The compelling conclusion is that these three salt windows introduced an unacceptable level of degradation of the optical performance of the system, dropping the Strehl ratio to 0.2 from an expected 0.5. In conjunction with the vendor, vigorous studies were initiated to study the problem and improve the optical quality of the large salt windows in their mounts.

Another interesting example of an application of this type of analysis had to do with the effects on optical performance due to the double passed salt window to enable the use of saturable absorbers to prevent parasitic oscillations.⁵ The conclusions reached can be stated by examining Figure 6. Considering the diameter at the target plane of 200 microns, the encircled energy is 86 percent (and the Strehl ratio of 0.49) for the case without the saturable absorber and 67.5 per cent (Strehl ratio of 0.16) for the case with the saturable absorber. This would tend to indicate that the case without the saturable absorber is the better choice. However, in absolute terms, because of the 1200 joules attainable with the saturable absorber as opposed to 600 joules attainable without saturable absorber, the peak irradiance is only slightly lower for the case using the saturable absorber* and the actual amount of useful energy** is considerably greater. Also, the lower value of Strehl (.16) actually is a distinct advantage here in that the energy density distribution is far more uniform than that for the case without saturable absorber usage.

Conclusions

The analysis techniques and methods used to characterize the various optical components and predict the performance of the LASL CO₂ laser fusion systems appear to be quite useful in understanding and optimizing the optical performance of these complex systems.

Encircled energy and beam quality measurements have not yet been performed in the Helios system to the levels of accuracy needed to verify the computations reported in this paper. However, burn paper measurements made in the Helios system tend to support these results. Also, computations of beam sizes and intensity levels for various experiments near the target focal plane have been experimentally verified to work well. Similar computations for the Gemini CO₂ laser fusion system have been experimentally verified. This excellent agreement between the computations and the experiments is reported in another paper in these proceedings.⁵

It appears that these programs, as well as the approach described in this paper, can be successfully used in the analysis, understanding, and optimization of similar complex, coherent electro-optical systems which defy conventional approaches based on ray tracing.

References

1. An excellent description of the Zernike polynomials, their properties and use in optics can be found in "Principles of Optics" by M. Born and E. Wolf, published by the MacMillan Company, New York.
2. These programs are: A) CDFL - computer determined fringe locator written by W. S. Hall of the LASL. B) FRINGE - the generic name for an interferometric analysis program originating from the Univ. of Arizona, and developed especially by J. Loomis. C) LOTS (Laser Optical Transport System) - a diffraction propagation code tailored to the LASL laser fusion systems - developed by G. Lawrence of the Univ. of Arizona in conjunction with the Laser Division of LASL.
3. For an example, see the article "Unique Problems and a Possible Novel Optical Design Approach for the Design and Assembly of CO₂ Laser Fusion Systems" V. K. Viswanathan, SPIE Proceedings, Vol. 147 (1979) on computer-aided optical design.
4. These results were discussed in the talk TuC 4-1 "Optical Analysis and Predictions for the LASL Eight Beam Laser Fusion System," V. K. Viswanathan, Inertial Confinement Fusion Meeting, CLEOS, San Diego, CA, Feb. 1979.
5. "Optical Performance of the Gemini CO₂ Laser Fusion System," V. K. Viswanathan, J. J. Hayden and I. Liberman, Paper #22-13, LASL Conference on Optics '79, Los Alamos, NM, May 23 - 25, 1979.

* 4.1×10^7 J/sq. cm vs. 5.6×10^7 J/sq. cm.

**910 J vs. 516 J.

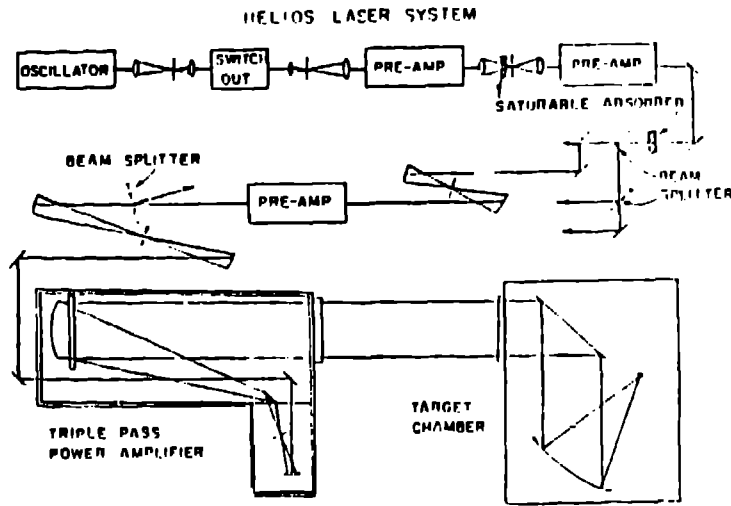


Figure 1.

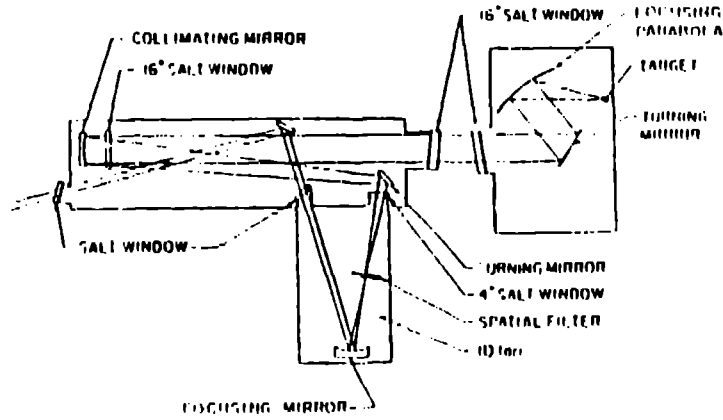


Figure 2.

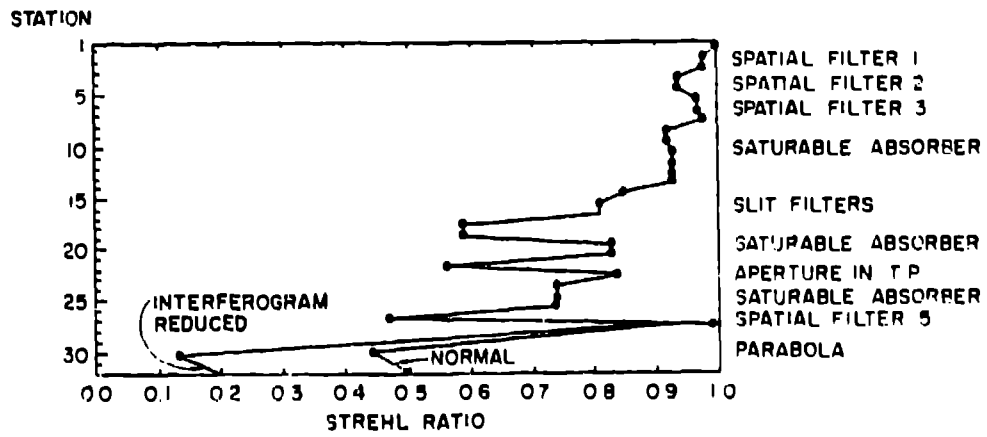


Figure 3

SYSTEM-OPTICAL DESCRIPTION

NO.	RADIUS (CMS)	CLEAR APERTURE RADIUS (CMS)	TO NEXT ELEMENT (CMS)	R. M. S. OPTICAL PATH DIFFERENCE FOR EACH ELEMENT AT 10.6 MICRONS (IN UNITS OF λ)			DESCRIPTION
				A	B	C	
1	78	1	39	-	-	-	FOCUSING MIRROR
2	•	.025	97.5	-	-	-	SPATIAL FILTER
3	•	1.4	18.1	.016	.032	.007	SALT WINDOW
4	•	5	47.2	.028	.056	.028	15° TURNING MIRROR
5	•	20.3	100	.033	.066	.031	SATURABLE ABSORBER SALT WINDOW
6	1326	19.7	100	.04	.08	.04	COLLIMATING MIRROR
7	•	20.3	488.3	.033	.066	.031	SATURABLE ABSORBER SALT WINDOW
8	•	20.3	198.1	.033	.066	.031	IPA EXIT SALT FLAT
9	•	20.3	121.9	.033	.066	.031	TARGET CHAMBER SALT FLAT
10	•	20.3	103.6	.028	.056	.03	15° TURNING MIRROR
11	154.52	20.3	77.26	.024	.048	.024	FOCUSING PARABOLA
12	•	.025	FOCAL PLANE				TARGET PLANE

*In the actual computation the actual size of the interferogram as well as the size of the beam at each element has been taken into account

Figure 4.

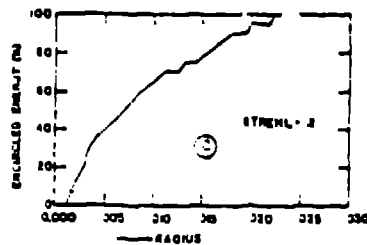
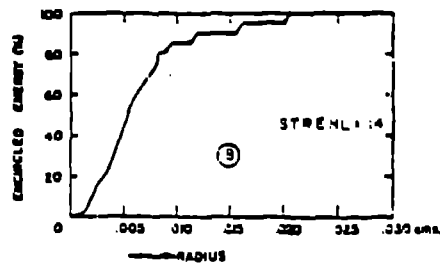
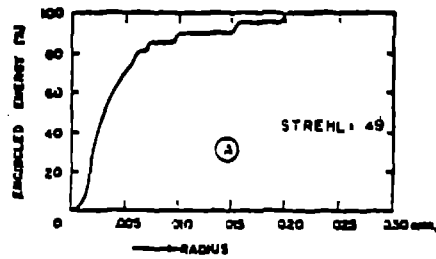


Figure 3. Encircled Energy

190-46

<u>DIAMETER OF TARGET</u>	<u>500 JOULES WITHOUT SAT ABSORBER</u>	<u>1000 JOULES WITH SAT ABSORBER</u>
100 μ m	300 (67%)	400 (40%)
120 μ m - 2 AIRY DISCS	400 (80%)	500 (50%)
200 μ m	450 (90%)	675 (67.5%)
300 μ m	475 (95%)	310 (31%)

<u>PEAK IRRADIANCE</u>	<u>$4 \times 10^7 \frac{\text{JOULES}}{\text{cm}^2}$</u>	<u>$3.3 \times 10^7 \frac{\text{JOULES}}{\text{cm}^2}$</u>
<u>STREHL</u>	0.5	0.2

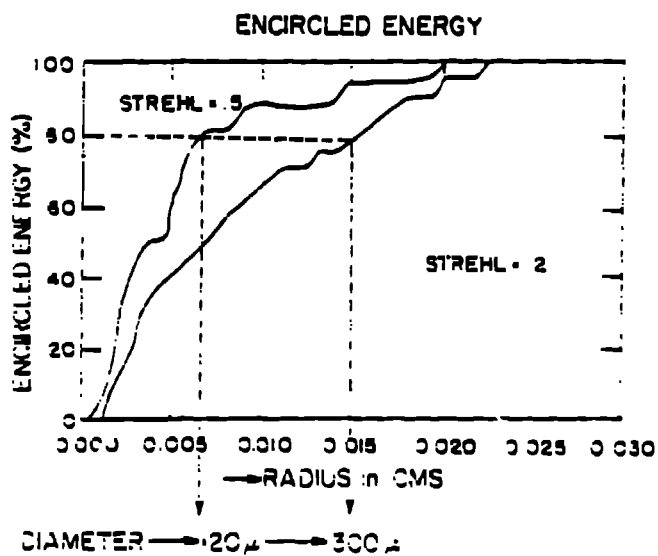


Figure 6.